Eur Biophys J (2008) 37:573–582
DOI 10.1007/s00249-008-0266-3

ORIGINAL PAPER

Dynamics of well-folded and natively disordered proteins in solution: a time-of-flight neutron scattering study

A. M. Gaspar · M.-S. Appavou · S. Busch · T. Unruh · W. Doster

Received: 13 October 2007 / Revised: 19 December 2007 / Accepted: 8 January 2008 / Published online: 29 January 2008

Abstract Casein proteins belong to the class of natively disordered proteins. The existence of disordered biologically active proteins questions the assumption that a well-folded structure is required for function. A hypothesis generally put forward is that the unstructured nature of these proteins results from the functional need of a higher flexibility. This interplay between structure and dynamics was investigated in a series of time-of-flight neutron scattering experiments, performed on casein proteins, as well as on three well-folded proteins with distinct secondary structures, namely, myoglobin (α), lysozyme (α/β) and concanavalin A (β). To illustrate the subtraction of the solvent contribution from the scattering spectra, we used the dynamic susceptibility spectra emphasizing the high frequency part of the spectrum, where the solvent dominates. The quality of the procedure is checked by comparing the corrected spectra to those of the dry and hydrated protein with negligible solvent contamination. Results of spectra analysis reveal differences in motional amplitudes of well-folded proteins, where β-sheet structures appear to be more rigid than a cluster of α-helices. The disordered caseins display the largest conformational displacements. Moreover their global diffusion rates deviate from the expected dependence, suggesting further large-scale conformational motions.

Advanced neutron scattering and complementary techniques to study biological systems. Contributions from the meetings, "Neutrons in Biology", STFC Rutherford Appleton Laboratory, Didcot, UK, 11–13 July and "Proteins At Work 2007", Perugia, Italy, 28–30 May 2007.

A. M. Gaspar (✉) · M.-S. Appavou · S. Busch · T. Unruh · W. Doster (✉)
E13, Physik Department, Technische Universität München, Lichtenberg str 1, 85747 Garching bei München, Germany
e-mail: agaspar@frm2.tum.de

W. Doster
e-mail: wdoster@ph.tum.de

A. M. Gaspar · T. Unruh
FRM II Forschungsneutronenquelle Heinz Maier-Leibnitz, Technische Universität München, Lichtenberg str 1, 85747 Garching bei München, Germany

Introduction

The function of proteins is essentially determined by their three-dimensional structure, and thus by the protein specific amino acid sequence. Most proteins assume a unique structure in their native state. There are, however, proteins that are largely disordered in their "functional state", lacking any secondary structural motifs (Wright and Dyson 1999; Uversky et al. 2000; Uversky 2002; Smyth et al. 2001). Nevertheless these proteins are found to carry out important biological functions, such as, in the case of the milk caseins, the binding and transport, of calcium mainly in the form of protein-bound nano-clusters (Qi et al. 2001; Farrell et al. 2002, Smyth et al. 2004).

The caseins comprise a family of four proteins (α_1-, α_2-, β- and κ-casein), representing about 80% of the total milk proteins (Walstra and Jenness 1984; Wong et al. 1996). Of these, α_1- and α_2-caseins represent 40 and 10%, respectively, and are together referred to as α-casein, while β-casein represents another 40% and κ-casein the remaining 10%. None of the four kinds of caseins has a highly organized secondary structure, with the different methods of analysis suggesting little more than a few short stretches of α-helix or β-sheet structure in them (Walstra and Jenness 1984; Wong et al. 1996; Sawyer and Holt 1992; Smyth et al. 2001; Farrell et al. 2001; Syme et al. 2002). As an approximation, the caseins can be

thought of as block copolymers consisting of blocks of high levels of hydrophobic and hydrophilic amino-acid residues (Horne 2002).

In the milk, the caseins exist associated with the colloidal particles known as the "casein micelle" whose shape is that of a roughly spherical, fairly swollen particle of diameter in the range of 50–300 nm (Walstra and Jenness 1984, Hansen et al. 1996; Kruif 1999; Holt et al. 2003; Gebhardt et al. 2005; Marchin et al. 2007). Also the individual caseins exhibit tendencies to self-associate and are known to form, in aqueous solution, small micelles of radius of the order of 8–12 nm, depending on several factors like, for instance, the protein concentration (Walstra and Jenness 1984; Wong et al. 1996; Leclerc and Calmettes 1997, 1998; Alaimo et al. 1999; Farrell et al. 1999; O'Connell et al. 2003; Dauphas et al. 2005; Euston and Horne 2005).

The evolutionary persistence of these so-called "natively disordered" proteins, the fact that they can have important biological functions, and their strong tendency to associate raise intriguing questions about the role of protein disorder in biological processes. Such a parameter has in the past received little attention from the scientific community but, since it has been established that the deposition of some natively disordered proteins is related to the development of several neuro-degenerative disorders (Uversky et al. 1999), a growing awareness of its importance was observed.

A hypothesis generally put forward in discussions is that natively disordered proteins might need a high structural flexibility to perform their function (Uversky 2002). In the investigations discussed below, we analyze this interplay between structure and dynamics by dynamic neutron scattering. To our knowledge these are the first experiments of this type performed on natively disordered proteins, despite the already proven potential of neutron scattering techniques in the investigation of protein dynamics (Lechner and Longeville 2006; Doster and Settles 2005).

In particular, we investigated the repercussions that the differences in, or absence of, the secondary structure of proteins have on motions occurring in time scales of the order of pico- to nano-seconds, accessible by time-of-flight quasi-elastic neutron scattering of cold neutrons (Bee 1988). Those motions correspond mainly to rotational motions of the amino-acid side chains, for which the secondary structure of the protein is believed to play a more relevant role than its tertiary or quaternary structure. Hence, the measurements were performed not only on the three natively disordered proteins mentioned above (α-, β- and κ-casein), but also on three well-known proteins of well-defined three-dimensional structure but distinct secondary structures, myoglobin, a protein mainly composed of α-helices; concanavalin A, a protein mainly composed of β-sheets, and lysozyme, a protein composed of both α and β motifs (see, e.g. Branden and Tooze 1999).

For technical reasons related to the experimental method used in this study, each of the proteins were studied in aqueous solution, as well as in the form of dry and hydrated powders. In the case of the spectra of protein powders, one does not have to deal with a significant solvent contribution and, in addition, the long-range motions of the protein are inhibited; hence the scattered signal allows for a direct analysis of the protein internal motions. This is not the case for the spectra of proteins in solution, however, in this situation, proteins are closer to the physiological conditions in which we are ultimately interested. Studying the proteins in both powder and solution forms eases data-analysis and interpretation. In this manuscript, the results obtained for the powder samples will be discussed only insofar as they provide support for the procedure used to extract the protein spectra from the data collected from the protein solutions. The method adopted, making use of the dynamical susceptibilities instead of the dynamical structure factor spectra, takes advantage of the wide dynamical range and high signal to noise ratio available at time-of-flight spectrometers.

Materials and methods

Samples

Essentially salt-free lyophilized powders of α-, β- and κ-caseins from bovine milk (23.2, 23.6 and 19.0 kDa, respectively) as well as horse heart myoglobin (17.0 kDa), chicken egg white lysozyme (14.7 kDa) and jack bean concanavalin A (25.5 kDa) were purchased from Sigma-Aldrich Co.

For the preparation of the protein powders, each of the proteins was either dissolved in D_2O or exposed to a D_2O-saturated atmosphere to exchange the labile hydrogen atoms. After this process, dry powders of each of the individual proteins were obtained by placing each of the samples for more than 48 h in a sealed environment in the presence of silica gel. The dryness of the powders obtained in this way was confirmed by further submitting them to high vacuum conditions, after which no reduction in their masses was observed. To avoid posterior hydration or H-contamination, all additional manipulations of the samples were performed in a glove box filled with argon.

Hydrated powders of each of the individual proteins were obtained rehydrating the corresponding dry powders by vapor adsorption of D_2O up to a hydration level of $\sim 0.4\, g_{D_2O}/g_{protein}$. The water content of the samples was determined by weighing. This was done not only before exposure to the neutron beam, but also controlled after that to exclude the possibility of dehydration during data acquisition.

The solution samples were obtained dissolving each of the individual protein powders separately in D_2O, at a concentration of $\sim$50 $mg_{protein}/ml_{solution}$, and concentrating these solutions by centrifugation using centricon filters from Millipore with a 3 kDa molecular weight cutoff, up to a concentration of $\sim$100 $mg_{protein}/ml_{solution}$. The concentration of the solutions obtained this way was controlled by UV absorption spectroscopic measurements (except for the myoglobin solution) and by removing and subsequently drying small volumes of sample, weighing the resultant amounts of dry protein.

In such aqueous solutions, myoglobin and lysozyme exist as monomers of hydrodynamic radius 1.9 and 1.7 nm, respectively (Perez et al. 1999), while concanavalin A exists in dimers of hydrodynamic radius 3.0 nm (Sawyer et al. 1975; Ahmad et al. 2007); α-, and κ- caseins are believed to form micelles of radius of the order of 8–12 nm (Alaimo et al. 1999; Farrell et al. 1999), whereas in the case of β-casein, at room temperature, a mixture of monomers of hydrodynamic radius 4 nm, and micelles, of hydrodynamic radius 8–12 nm is expected to be present (O'Connell et al. 2003). It should be noted, however, that the mentioned previous studies have been performed at much lower sample concentrations and that complementary photon correlation spectroscopy (PCS) experiments performed in our laboratory as a function of concentration appear to indicate a tendency of the micelles to become smaller upon increase of the concentration (Gaspar et al. 2006). Of importance for this study is the fact that even if all the caseins were present in solution only as monomers, their hydrodynamic radius of about 4 nm would still be higher than the hydrodynamic radius of the three well-folded proteins in solution, 2–3 nm.

Measurements

The experiments were performed at the time-of-flight spectrometer TOFTOF at FRM II (Zirkel et al. 2000; Gaspar 2005; Unruh et al. 2007), choosing a wavelength of 6 Å for the incident neutrons and a chopper speed of 12,000 rpm, which corresponds to an instrument resolution at the elastic line of approximately 30 μeV (HWHM), and hence to a time scale of 22 ps.

The momentum versus energy transfer region probed with this instrument configuration is displayed in Fig. 1. As can be seen, such a configuration probes a wide spectral range on the energy gain side, extending far beyond the quasi-elastic region of the spectrum (commonly defined as the region from −1 to 1 meV), and is in fact only limited in energy gain value by the point at which the sample signal decreases, due to the exponential decay of the Bose-population factor, below instrumental noise. Given the excellent signal to noise ratio at TOFTOF, this situation

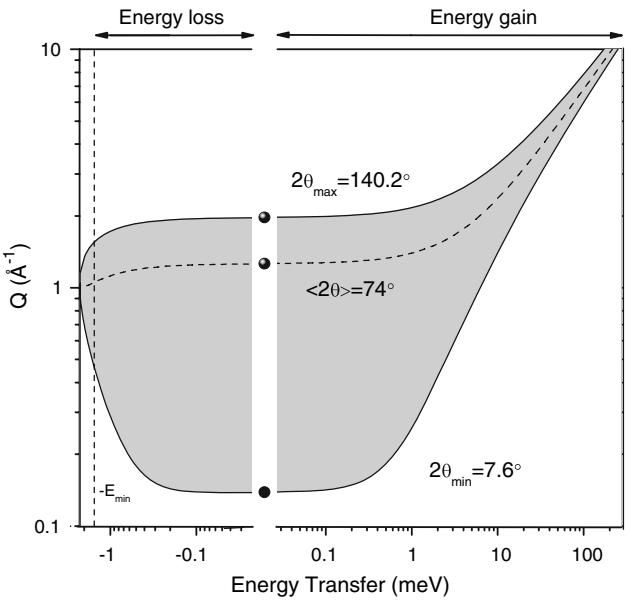

Fig. 1 Momentum versus energy transfer region, probed by the measurements performed at TOFTOF. The *dotted line* denotes the angle-averaged spectra. The *vertical dashed line* represents the maximum energy loss accessible by the measurements, which is defined by the frame overlap ratio chosen, for further details report, to Gaspar 2005

was, for our measurements, only reached at an energy transfer of about 200 meV.

All the samples were studied at room temperature (293K) in hollow aluminum containers of 11.25 mm external radius (with walls of 0.25 mm thickness) and defining a sample layer thickness of 0.5 mm. Such a sample container allows using the full angular range available at the instrument and simplifies geometrical corrections, at the expense of the introduction of a small angle dependent worsening of the resolution (Gaspar 2005).

Each of the proteins was individually studied in the form of dry and hydrated powders (of hydration <0.05 $g_{D_2O}/g_{protein}$ and ~ 0.4 $g_{D_2O}/g_{protein}$, respectively), as well as in deuterated aqueous solution (with a protein concentration of $\sim$100 $mg_{protein}/ml_{solution}$). The amount of protein in the beam was about 250 mg for dry powders, 200 mg for hydrated powders and 150 mg for proteins in solution. The average measuring time per spectrum was 8 h for the liquid samples and 6 h for the powder samples. Measurements were also made, at the same temperature, of an empty container, of pure D_2O, and of a vanadium sample, with the same geometry and thickness as the samples.

Data-reduction and analysis

Data-reduction and analysis was performed using the program FRIDA (Wuttke 2006). The measured time-of-

flight spectra were normalized to the monitor and vanadium standard, converted from time-of-flight to energy transfer (E) and from $\partial\sigma/(\partial E \partial 2\theta)$ to $S(2\theta,E)$. The data were also corrected for differences in detector efficiency for neutrons of different final energies. The sample signal was then obtained by subtraction of the empty can signal taking into account the appropriate self-absorption corrections (Wuttke 1991; Bee 1988; appendix of Chap. 4).

For the solution samples, the solvent contribution was subtracted from the sample signal, taking into account the volume fraction of bulk solvent "α" in the protein solution (Perez et al. 1999; Fitter 2006):

$$S_{\text{prot solution}}(2\theta,E) = S_{\text{total solution}}(2\theta,E) - \alpha S_{D_2O}(2\theta,E) \quad (1)$$

where "α" was obtained, subtracting from the total D_2O volume fraction [itself directly calculated from the known solution concentration and the average protein density (Fischer et al. 2004)], the parcel corresponding to the first hydration-shell (considered complete at a hydration of $0.4\, g_{D_2O}/g_{\text{protein}}$).

Finally, to facilitate a direct comparison of the spectra of different proteins, the spectra were also normalized to the total number of counts collected at the TOFTOF detectors, considered to be roughly proportional to the total sample scattering cross section.

For the inspection of the structural information, static structure factors were obtained integrating the two-dimensional spectra over the entire energy transfer range accessible (see Fig. 1)

$$S(Q) = \int_{-E_{\min}}^{\infty} S(2\theta,E)\mathrm{d}E \quad (2)$$

with Q approximated to its value at the elastic line $Q_0 = (4\pi/\lambda)\sin\,\theta$, as usually done with data collected at diffraction instruments.

For the inspection of the vibrational information, one-dimensional spectra were obtained, summing the spectra collected at the different scattering angles

$$S(E) = \sum_{2\theta} S(2\theta,E). \quad (3)$$

Spectral information contained at higher energy transfer values was then enhanced by dividing $S(E)$ by the Bose population factor $n(E) = (e^{E/kBT} - 1)^{-1}$, with k_B representing the Boltzmann constant, thereby arriving to a dynamical susceptibility function

$$\chi''(E) = S(E)/n(E). \quad (4)$$

In such angle averaged spectra, i.e. both in $S(E)$ and $\chi''(E)$, to each value of E corresponds a slightly different average Q value, as is usually the case for spectra collected at inelastic neutron scattering instruments. In the case of the TOFTOF measurements discussed here, this relation is represented in Fig. 1 by the dotted line corresponding to the average scattering angle $\langle 2\theta \rangle = 74°$.

For the analysis of the diffusive motions of the proteins, that is the motions contributing to the broadening of the elastic line (or, in other words, to a reduction in scattering at $E = 0$) the spectra were grouped into constant Q slices of half-width 0.05 Å^{-1}. Analysis then included fitting independently the quasi-elastic region (considered to be defined by $|E| < 1$ meV) of each constant-Q spectrum with an empirical expression.

For proteins in solution, for which both localized (internal) and long-range (global) diffusive motions are present, the simplest expression able to describe the observed spectra was used (Bee 2003):

$$S(Q,E) = P(Q)\left\{\frac{1}{\pi}\frac{\Gamma_{\text{dif}}(Q)}{E^2+\Gamma_{\text{dif}}^2(Q)} \otimes \left[A_0(Q)\delta(E) + \frac{(1-A_0(Q))}{\pi}\frac{\Gamma_{\text{int}}(Q)}{E^2+\Gamma_{\text{int}}^2(Q)}\right] + B(Q)\right\} \otimes S_{\text{res}}(Q,E) \quad (5)$$

where $\otimes$ represents the convolution operation in energy space, $S_{\text{res}}(Q,E)$ is the resolution function (vanadium measurement), $\Gamma_{\text{int}}(Q)$ and $\Gamma_{\text{dif}}(Q)$ are half widths at half maximum (HWHM) of two Lorentzian functions, representing the internal and the global motions of the protein, respectively, $A_0(Q)$ is the term called "elastic incoherent structure factor" characterizing the geometry or amplitude of restricted motions, $B(Q)$ is a background due to vibrational motions and $P(Q)$ is a scaling factor that includes the Debye–Waller term.

Results and discussion

Solvent subtraction procedure

Figure 2 illustrates, for myoglobin, the solvent subtraction procedure, performed on the measurements of the proteins in solution. There, the solvent and protein contributions to the total signal are displayed and the protein terms compared with the equivalent ones directly accessed from the

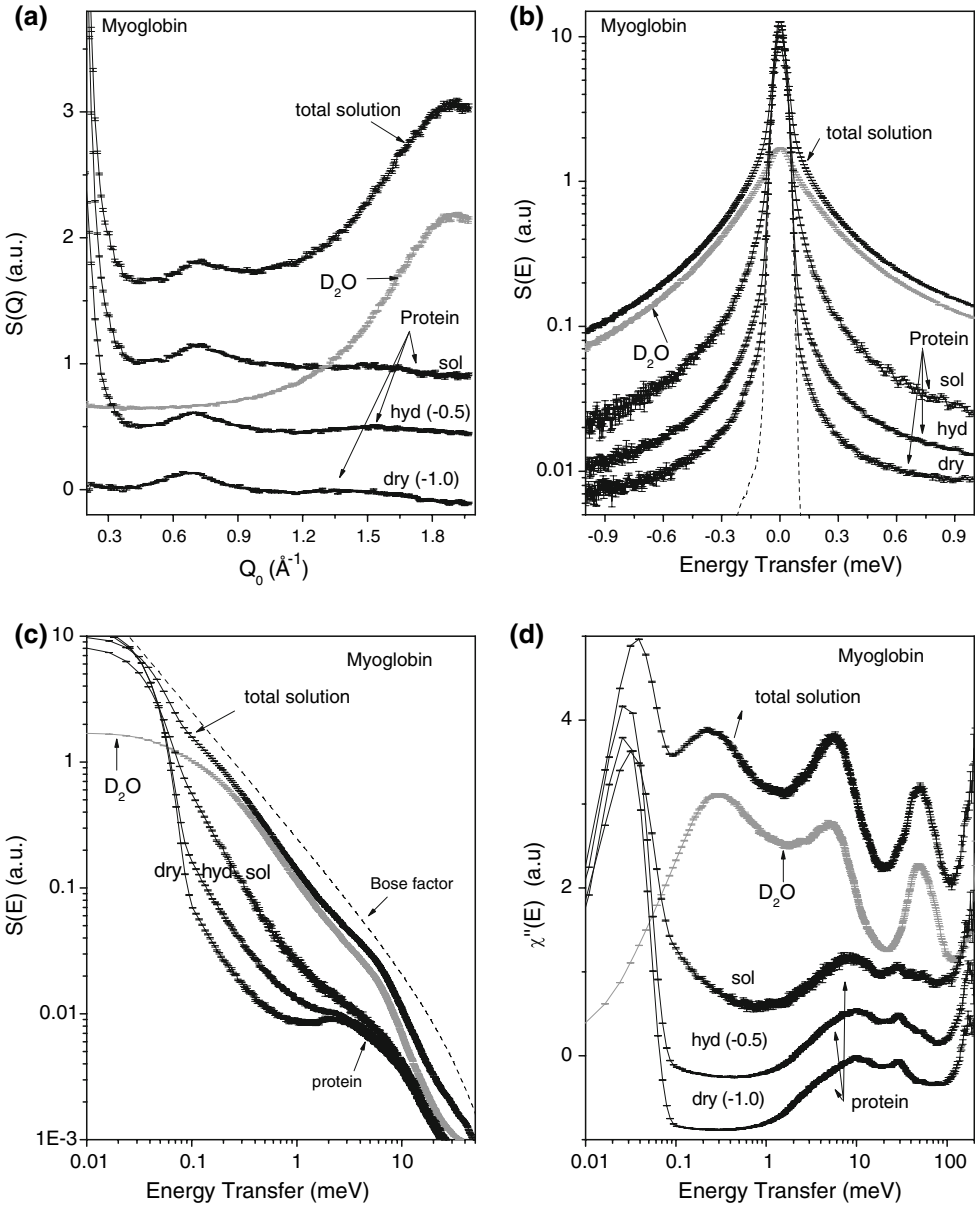

Fig. 2 Illustration of the solvent subtraction procedure performed on measurements of proteins in solution for one of the samples investigated, Myoglobin. Protein terms extracted from the solution data are compared with the equivalent ones directly accessed from the experiment for the powders of the same protein. **a** Static structure factors, **b** and **c** angle averaged spectra $S(E)$ in different graphical representations and **d** dynamical susceptibility $\chi''(E)$. The values (-0.5) and (-1.0) on graphs **a** and **d** correspond to a shift of the spectra. In the figures, the annotations "*dry*", "*hyd*" and "*sol*" identify protein spectra obtained for the "dry protein power", the "hydrated protein powder" and the "solution", respectively

experiment for the powders (both dry and hydrated). The different plots display the different regions of the dynamic range accessible by the experiment, namely they display the static structure factors $S(Q)$, in (a), the angle averaged spectra $S(E)$, in different graphical representations (b, c), and the dynamical susceptibility $\chi''(E)$, in (d).

In plots 2a, 2c and 2d, structural, quasi-elastic and vibrational features, characteristic of the solvent can be identified as distinct features. This makes those representations particularly useful for the evaluation of the success of the separation of the solvent and protein terms in solution data. The plot of the dynamical susceptibilities $\chi''(E)$ is especially useful, since it emphasizes the high frequency range of the spectrum. There the solvent term dominates the spectra, in particular for energy transfer values higher than 1 meV (i.e. across the vibrational region). It is thus convincing that the protein term shows no contamination by the solvent dynamical features after subtraction, resembling remarkably the spectra obtained directly from measurements on the powders. The same procedure when applied to the other proteins led to results of similar quality.

In contrast, in the quasi-elastic region (here considered the region from -1 to 1 meV), the spectra of the dry and hydrated protein, and that of the protein in solution, differ from each other (as shown in plots 2b, c and d). Therefore, using only the information plotted in Fig. 2b) does not allow a thorough inspection of the success of the separation of the solvent and protein contributions in solution data.

The quasielastic scattering term increases from the dry, to the hydrated, to the solvated state. Whether the

displacement amplitude or the fluctuation rate or both increase with hydration is not easy to decide. It has been shown that the hydrated state of myoglobin involves continuous small-scale motions, while in the dehydrated system essentially discontinuous rotational jumps of methyl groups prevail (Doster and Settles 2005). In the solvated state, further breathing motions could occur or the viscosity of water decreases with solvation leading to faster conformational relaxation (Doster and Settles 2005). It should also be noted that the differences observed in the quasi-elastic spectra of the same protein in the different states occur not only because of the diffusive motions within the protein (internal motions), but also because the center of mass diffusion of the entire protein (global motions), is not the same in the three different situations. Therefore, quasi-elastic scattering provides us with the means to study those diffusive motions. In the rest of this contribution we will concentrate on the analysis of these differences in the quasi-elastic spectra of different proteins in solution.

Analysis of the $S(E)$ of different proteins in solution

The normalized (to the total number of counts) angle-averaged spectra $S(E)$ of the different proteins in solution are compared in Fig. 3, highlighting the spectral regions of elastic and quasi-elastic scattering. In fact, for proteins in solution, there is no purely elastic scattering, since the entire proteins are free to diffuse. This leads to a global broadening of the elastic line and of the quasi-elastic line, itself due to the internal motions of the proteins, as the result of the convolution of the two types of spectral broadening. Still, for a matter of convenience, the terms *region of elastic scattering* and *region of quasi-elastic scattering* are used throughout this document as referring to the regions over which the instrumental resolution defines to a large extent the width of the scattering curve (displayed in Fig. 3a) and the region over which the broadening of the elastic line can be analyzed without being contaminated by vibrational features (i.e. the region from -1 to 1 meV displayed in Fig. 3b).

The figure shows spectral differences between the various proteins in the elastic and quasi-elastic regions: less intense scattering in the elastic region (Fig. 3a) is compensated by a higher level of the spectral tail at 1 meV (Fig. 3b), in agreement with the sum rule and the normalization procedure adopted. As previously mentioned, the differences observed among the spectra of different proteins in solution may result from differences in the center of mass diffusive motions (global motions), as well as from differences in the internal motions of the different proteins. If they could be attributed only to the global motions of proteins, then the highest scattering intensity at $E = 0$ would

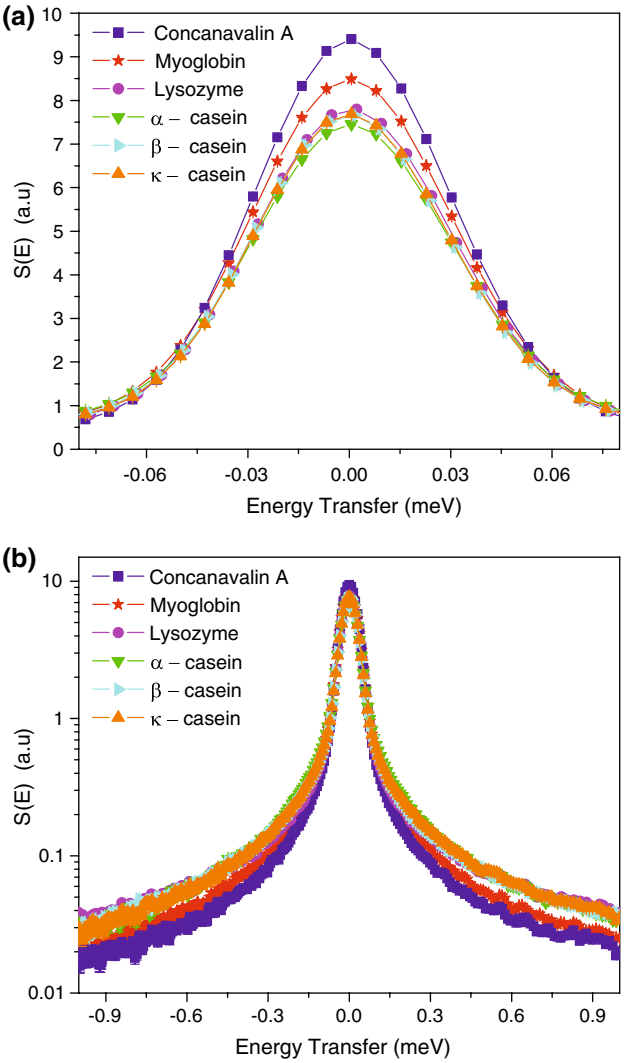

Fig. 3 Normalized angle averaged spectra $S_{\text{prot\_solution}}(E)$ obtained for the different proteins in solution, displayed over the spectral region corresponding to elastic scattering **a** and over the spectral region corresponding to quasi-elastic scattering **b**)

be the scattering from the protein with the largest hydrodynamic radius, since in that case the protein global motions would be the slowest and hence the broadening of the elastic line would be the smallest. This relation is indeed verified for the spectra of lysozyme, myoglobin and concanavalin A, for which indeed $R_{\text{Lys}} < R_{\text{Myo}} < R_{\text{ConcA}}$ appears translated into $S_{\text{Lys}}(0) < S_{\text{Myo}}(0) < S_{\text{ConcA}}(0)$. However, it is not verified when comparing the spectra of these three proteins with the spectra of the three caseins. In fact, for the caseins, the elastic scattering intensities fall below the level of the one of lysozyme, whereas one would expect those intensities to be at a level considerably higher than the one observed for concanavalin A. This result is a direct indication that the differences between the quasi-elastic spectra of well-folded and disordered proteins do not result only from the differences in their global motions.

In the following, a detailed analysis of the Q-dependence of this effect is pursued performing fits to constant-Q spectra and determining the parameters characterizing the global as well as the internal motions of proteins.

Analysis of the fit results

For each protein, the quasi-elastic region of each constant-Q spectrum was fitted independently using the empirical expression (5). This expression consists of the simplest expression able to describe spectra resulting from both localized (internal) and long-range (global) diffusive motions (Bee 2003). The long-range (global) diffuse motions are included in a Lorentzian term (of HWHM $\Gamma_{dif}(Q)$) which appears convoluted with another term due to the localized (internal) motions. This latter term contains a single characteristic time rate (obtained from the width $\Gamma_{int}(Q)$ of a second Lorentzian term), and hence carries the assumption that all the internal motions resolved by the spectrometer do not have characteristic time rates significantly different from that average value.

Figure 4 displays in logarithmic scale, for one of the proteins investigated and for three of the Q-values considered in the analysis, the excellent quality of the fits produced. The results obtained for the other Q-values and for all the proteins exhibit similar fit quality.

Figure 5 displays the fit parameters characterizing the internal (Fig. 5a) and global (Fig. 5b) motions of the different proteins in solution. Specifically, Fig. 5a displays $A_0(Q)$, and $\Gamma_{int}(Q)$, which together represent the protein internal motions, whereas Fig. 5b displays $\Gamma_{dif}(Q)$, the HWMH of the Lorentzian representing the center of mass diffusion of the protein.

Concerning the internal motions (Fig. 5a), relevant differences are observed in the elastic incoherent structure factor $A_0(Q)$ of the different proteins, whereas this appears to be not the case for $\Gamma_{int}(Q)$. It should however be noted that the latter parameter (which, as expected for internal motions, appears as a fairly Q-independent parameter) has proved to be a quite weak parameter, since fixing it to $\Gamma_{int} = 0.15$ meV for all the proteins and all Q-values does not lead to significant differences in the other parameters. The opposite was observed for $A_0(Q)$, which has proved to be a quite robust parameter.

The differences observed for the different proteins suggest that the secondary structure of proteins plays a relevant role in determining the internal dynamics in solution, probably not so much concerning its characteristic time, but rather concerning the fraction of protons actually involved in those motions, as well as the amplitudes of those motions. It should be noted, however, that in the simple expression adopted, the distribution of proton motions resolved by the spectrometer are also implicitly considered to be equivalent for the different proteins. Alternatively, the distribution of rates could be different for the different proteins, which would then be differently resolved by the spectrometer. The second case postulates a rate distribution, which is not included in the expression considered, but which could, at least partially, contribute to some of the differences observed in the $A_0(Q)$ of different proteins. In any case, proteins composed mainly of β-sheets appear to be less flexible, followed by proteins composed mainly of α-helices and then by those composed of a mixture of α and β-motifs, the unstructured proteins being in fact the most flexible ones. Such a trend is in agreement with what had already been suggested by molecular

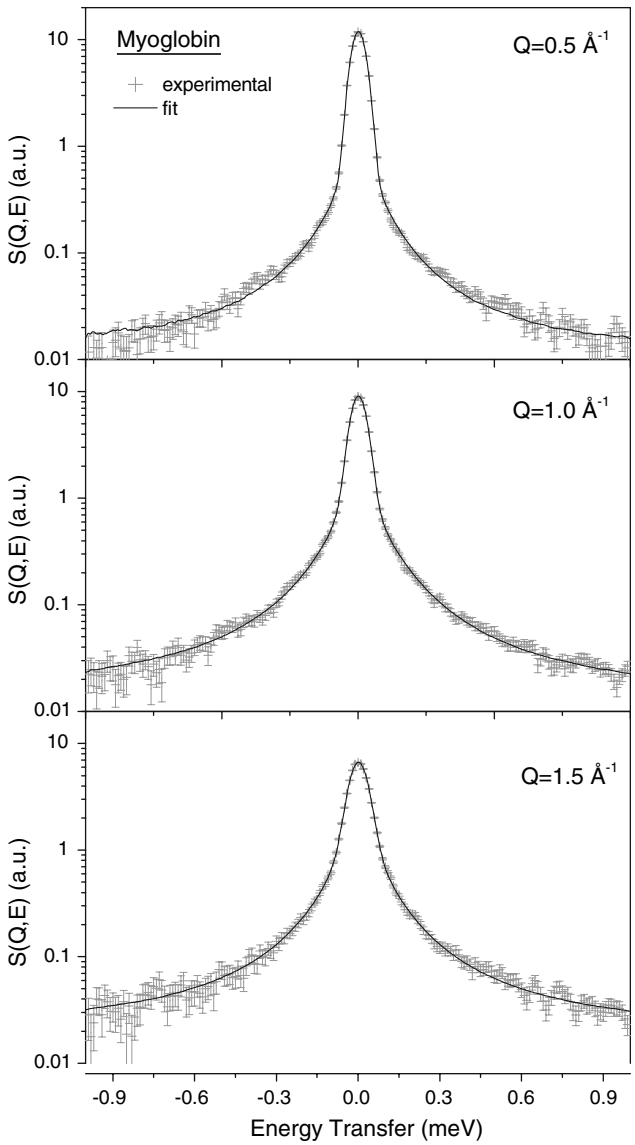

Fig. 4 Three of the constant-Q spectra $S(Q,E)$ and corresponding fit curves obtained for one of the samples investigated, Myoglobin, displayed for illustration of the quality of the fits

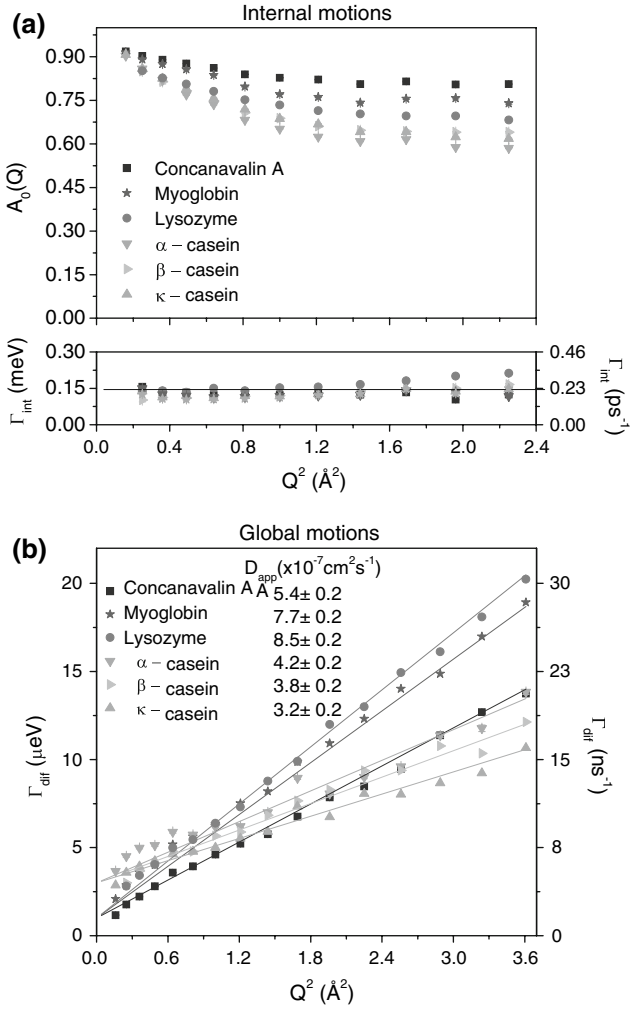

Fig. 5 Fit parameters characterizing the motions of the different proteins in solution. **a** Elastic incoherent structure factor $A_0(Q)$ and HWHM of the Lorentzian of larger width, attributed to the internal motions of the proteins. **b** HWHM of the Lorentzian of smaller width, attributed to the global motions of the proteins

dynamics simulations, for the well-folded proteins (Tarek and Tobias 2006).

Concerning the center of mass diffusion motions (Fig. 5b), $\Gamma_{dif}(Q)$ exhibits, as expected, a linear dependence on Q^2, allowing to determine apparent diffusion coefficients consistent either with the values published in the literature for these well-folded proteins (Perez et al. 1999, Busch et al. 2006) or with their known hydrodynamic radius (Sawyer et al. 1975; Ahmad et al. 2007). The diffusion coefficients determined for the casein proteins are also smaller than the ones determined for the well-folded proteins, in agreement with their larger radius in solution (see "Samples").

Nevertheless, the fitted lines do not intercept the origin. Instead an offset is observed concerning the point at which the fitted lines intercept the vertical axis (Fig. 5b). Although this offset could, in the case of the well-folded proteins, be attributed to artifacts due to the resolution limit of the spectrometer (i.e. forcing the line to go through the origin would not change significantly the results obtained), this is not the case for the caseins. For these proteins, the offset is about three times higher than that for the other proteins and forcing the fitted line to go through the origin would lead to unsatisfactory results (Fig. 5b).

The presence of this offset appears to suggest the presence of other internal motions (slower motions) of a characteristic time on the same scale as detected in Γ_{diff}, which then render the description of all the internal motions resolved by the spectrometer by a single average characteristic time inappropriate. Complication of the expression used for the fits does however not appear a viable route for more reliable or conclusive results, given the increase in free parameters that would result from that. In these conditions, extending the available data set to longer time scales by performing backscattering and spin-echo experiments appears to be a better solution (Bu et al. 2005, Busch et al. 2006, Doster and Longeville 2007).

Conclusions

Neutron time-of-flight spectra show, in the time-scales of pico- to nano-seconds, features consistent with a higher flexibility of natively disordered proteins, when compared to well-folded proteins of different secondary structure. In particular, the differences in dynamical behavior appear to be not only a higher fraction of moving hydrogen atoms (and/or larger amplitude motions), but also the presence of other motions in the time window of the spectrometer. The results also reveal differences in motional amplitudes of well-folded proteins, where β-sheet structures appear to be more rigid than a cluster of α-helices. Further studies, namely using neutron back-scattering and spin-echo techniques, will allow a better understanding of the physical phenomena at the origin of the differences in the dynamical behavior of natively disordered and well-folded proteins.

In addition, this contribution illustrates how intricate data-reduction and analysis procedures, such as those related to proteins in solution, can be eased and checked taking the entire dynamical range accessible by the instrument into consideration. In the case of the time-of-flight experiments reported here, this range was shown to extend far beyond the quasi-elastic region.

Acknowledgments A M Gaspar acknowledges the supported given by Fundação para a Ciência e Tecnologia in the form of a post-doc grant SFRH/BDP/17571/2004. The project was further supported by a grant of the Deutsche Forschungsgemeinschaft SFB 533. Tobias Unruh contributed with the construction and commissioning of the

TOFTOF instrument. Valuable discussions and continuous support by Prof. Winfried Petry, as scientific director of the FRM II and supporter of the project, are also gratefully acknowledged by A.M. Gaspar.

References

Ahmad E, Naeem A, Javed S, Yadav S, Hasan Kahn R (2007) The minimal structural requirement of concanavalin A that retains its functional aspects. J Biochem 142:307–315

Alaimo MH, Wickham ED, Farrell Jr HM (1999) Effect of self-association of α_s-casein and its cleavage fractions α_s-casein (136–196) and α_s-casein (1–197) on aromatic circular dichroic spectra: comparison with predicted models. Biochim Biophys Acta 1431:395–409

Bee M (1988) Quasielastic neutron scattering. Adam Hilger, London

Bee M (2003) Localized and long-range diffusion in condensed matter: state of the art of QENS studies and future prospects. Chem Phys 292:121–141

Branden C, Tooze J (1999) Introduction to protein structure, 2nd edn. Garland Publishing Taylor & Francis, London

Bu Z, Biehl R, Monkenbusch M, Richter D, Callaway DJE (2005) Coupled protein domain motion in Taq polymerase revealed by neutron spin-echo spectroscopy. PNAS 102:17646–17651

Busch S, Doster W, Longeville S, García Sakai V, Unruh T (2006) Microscopic protein diffusion at high concentration. MRS Bull Quasielastic Neutron Scattering Conf 2006:117–116

Dauphas S, Mouhous-Riou N, Metro B, Mackie AR, Wilde PJ, Anton M, Riaublanc A (2005) The supramolecular organization of β-casein: effect of interfacial properties. Food Hydrocolloids 19:387–393

Doster W, Longeville S (2007) Microscopic diffusion and hydrodynamic interactions of hemoglobin in red blood cells. Biophys J 93:1360–1368

Doster W, Settles M (2005) Protein–water displacement distributions. Biochim Biophys Acta 1749:173–186

Euston SR, Horne DS (2005) Simulating the self-association of caseins. Food Hydrocolloids 19:379–386

Fitter J (2006) Conformational dynamics measured with proteins in solution. In: Neutron scattering in biology: techniques and applications, Springer Biological Physics Series, Chap. 17

Farrell JR HM, Kumosinski TF, Cook PH (1999) Environmental influences on the particle sizes of purified kappa-casein: metal effect. Int Dairy J 9:193–199

Farrell Jr HM, Wickham ED, Unruh JJ, Qi PX, Hoagland PD (2001) Secondary structural studies of bovine caseins: temperature dependence of β-casein structure as analyzed by circular dichroism and FTIR spectroscopy and correlation with micellization. Food Hydrocolloids 15:341–354

Farrell Jr HM, Qi PX, Brown EM, Cooke EM, Tunich PH, Wickham ED, Unruh JJ (2002) Molten globule structures in milk proteins: implications for potential new structure-function relatioships. J Dairy Sci 85:459–471

Fischer H, Polikarpov I, Graievich AF (2004) Average protein density is a molecular-weight-dependent function. Protein Sci 13:2825–2828

Gaspar AM (2005) TOFTOF intensity and resolution functions, technical report, http://www.ph.tum.de/~agaspar/AG_toftofreport.pdf; arXiv:0710.5319v1(physics.ins-det)

Gaspar AM, Doster W, Gebhardt R, Petry W (2006) β-casein dynamics and association: quasi-elastic scattering studies, annual report of the chair E13 of the physics department of the Technische Universität München; unpublished results

Gebhardt R, Doster W, Kulozik U (2005) Pressure-induced dissociation of Casein Micelles, size distribution and the effect of temperature. Braz J Med Biol Res 38:1209–1214

Hansen S, Bauer R, Lomholt SB, Quist KB, Pedersen JS, Mortensen K (1996) Structure of casein micelles studied by small-angle neutron scattering. Eur Biophys J 24:143–147

Holt C, de Kruif CG, Tuinier R, Timmins PA (2003) Substructure of bovine casein micelles by small angle X-ray and neutron scattering. Colloids Surf A Physicochem Eng Asp 213:275–284

Horne DS (2002) Casein structure, self-assembly and gelation. Curr Opin Colloid Interface Sci 7:456–461

Kruif CG (1999) Casein micelle interactions. Int Dairy J 9:183–188

Leclerc E, Calmettes P (1997) Interactions in micellar solutions of β-casein. Physics B 234–236:207–209

Leclerc E, Calmettes P (1998) Structure of β-casein micelles. Physics B 241–243:1141–1143

Lechner RE, Longeville S (2006) Quasielastic neutron scattering in biology, partII: applications. In: Neutron scattering in biology: techniques and applications, Springer Biological Physics Series, Chap. 16

Marchin S, Putaux J-L, Pignon F, Leonil J (2007) Effects of the environmental factors on the casein micelle structure studied by cryo transmission electron microscopy and small-angle x-ray scattering/ultrasmall-angle X-ray scattering. J Chem Phys 126:045101

O'Connell JE, Grinberg VYa, Kruif CG (2003) Associatin behaviour of β-casein. J Colloid Interface Sci 258:33–39

Perez J, Zanotti J-M, Durand D (1999) Evolution of the internal dynamics of two globular proteins from dry powder to solution. Biophys J 77:454–469

Qi PX, Brown EM, Farrel Jr HM (2001) 'New-views' on the structure-function relationships in milk proteins. Trends Food Sci Technol 12:339–346

Sawyer L, Holt C (1992) The secondary structure of milk proteins and their biological function. J Dairy Sci 76:3062–3078

Sawyer WH, Dabscheck R, Nott PR, Selinger BK, Kuntz ID (1975) Hydrodynamic changes accompanying the loss of metal ions from concanavalin A. Biochem J 147:613–615

Smyth E, Syme CD, Blanch EW, Vasak M, Barron LD (2001) Solution structure of native proteins with irregular folds from Raman optical activity. Biopolymers 58:138–151

Smyth E, Clegg RA, Holt C (2004) A biological perspective on the structure and function of caseins and casein micelles. Int J Dairy Tech 57:121–126

Syme CD, Blanch EW, Holt C, Jakes R, Goedert M, Hecht L, Barron LD (2002) A Raman optical activity study of rheomorphism in caseins, synucleins and tau. Eur J Biochem 269:148–156

Tarek M, Tobias DJ (2006) Subnanosecond dynamics of proteins in solution: MD simulations and inelastic neutron scattering. In: Neutron scattering in biology: techniques and applications, Springer Biological Physics Series, Chap. 23

Unruh T, Neuhaus J, Petry W (2007) The high-resolution time-of-flight spectrometer TOFTOF. Nucl Instrum Methods Phys Res A 580:1414–1422 and erratum 585:201

Uversky VN (2002) What does it mean to be natively unfolded? Eur J Biochem 269:2–12

Uversky VN, Talapatra A, Gillespie JR, Fink AL (1999) Protein deposits as the molecular basis for amylosis. Parts I and II. Med Sci Monit 5:1001–1012 and 1238–1254

Uversky VN, Gillespie JR, Fink AL (2000) Why are 'natively unfolded' proteins unstructured under physiological conditions? Proteins 41:415–427

Walstra P, Jenness R (1984) Diary chemistry and physics. Wiley, New York

Wong DWS, Camirand WM, Pavlath AE (1996) Structures and functionalities of milk proteins. Crit Rev Food Sci Nutr 36:807–844

Wright PE, Dyson HJ (1999) Intrinsically unstructured proteins: re-assessing the protein structure-function paradigm. J Mol Biol 293:321–331

Wuttke J (1991) Data reduction for quasielastic neutron scattering, ILL internal report 91WU08T

Wuttke J (2006) FRIDA (fast reliable inelastic data analysis), http://sourceforge.net/projects/frida/

Zirkel A, Roth S, Schneider W, Neuhaus J, Petry W (2000) The time-of-flight spectrometer with cold neutrons at the FRM-II. Physica B 276–278:120–121